Res. Rep. Fac. Eng. Mie Univ., Vol. 26, pp. 11－21 (2001)


Original Paper

# Temper embrittlement in HAZ of Cr-Mo steel observed in SR-treated specimens

Hiroshi KAWAKAMI, Koreaki TAMAKI and Jippei SUZUKI
(Department of Mechanical Engineering)

(Received September 17, 2001)

Abstract

The temper embrittlment occurred in the heat affected zones (HAZs) of Cr-Mo steels tempered at the temperature range of 775 to 900K. The first to the fourth types of embrittlement appeared in order with an increasing tempering time when the HAZ specimen were tempered directly. The effect of SR treatment on temper embrittlement arising in HAZ of 2 1/4Cr-1Mo steel was investigated. The temper embrittlement was detected as the rise of the transition temperature, $vTr_{30}$. The first type of embrittlement disappeared completely and the second type did partially after SR treatment. The third type of embrittlement, which was typical intergranular type embrittlement, arose as well after SR treatment. This type was induced by the segregation of phosphorus in the prior-austenite grain boundary. The fourth type arose a little after the SR treatment. It was induced by the growth of carbide particles.

Key words: Temper embrittlement, Cr-Mo Steel, Heat affected zone, SR treatment, Transition temperature, Segregation of phosphorus, Intergranular fracture, Cleavage fracture.

## 1. Introduction

2 1/4 Cr-1Mo steel was used widely in the welded constructions such as the chemical reactors or the boilers, they were used in the temperature range around 825K. The temper embrittlement occurs occasionally in the heat affected zone (HAZ) of this steel when the welded constructions were used without the stress relief annealing (SR treatment). The authors have

observed four types of temper embrittlement in the direct-tempered HAZ specimens[1].

The welded constructions made by the thick sections of 2 1/4Cr-1Mo steel are used usually after the SR treatment by which the residual stress arising in the welded zone is removed[2]. The SR treatment may be useful as well for removing the temper embrittlement. This beneficial effect of SR treatment was confirmed in this research. The temper embrittlement was detected by the rise of the transition temperature, $vTr_{30}$. The types of embrittlement which arose in the SR-treated specimens were identified by referring to those in the direct-tempered specimens.

The metallurgical factors for inducing the temper embrittlement were discussed from the view points of the segregation of phosphorus in the prior-austenite grain boundary and the growth of carbide particles in ferrite matrix.

## 2. Experimental methods

### 2.1 Synthetic HAZ specimen

Table 1 shows the chemical compositions of 2 1/4Cr-1Mo steel. The synthetic HAZ specimen[1] was used. The microstructure of real HAZ was reproduced in a steel bar by a weld thermal cycle simulator. The microstructure of the HAZ specimen consists 20% martensite and 80% bainite.

**Table 1 Chemical composition of 2 1/4Cr-1Mo steel, mass%.**

| C | Si | Mn | P | S | Cr | Mo | As | N | $Al_{sol}$ |
|---|---|---|---|---|---|---|---|---|---|
| 0.14 | 0.16 | 0.56 | 0.006 | 0.002 | 2.17 | 0.90 | 0.004 | 0.0032 | 0.017 |

### 2.2 SR treatment and tempering

The thermal histories given to the SR-treated HAZ specimen is shown by the solid line in Fig.1. The dotted line shows the thermal histories of the original HAZ specimen[1]. The specimens were enclosed in a steel container during the SR treatment and tempering.

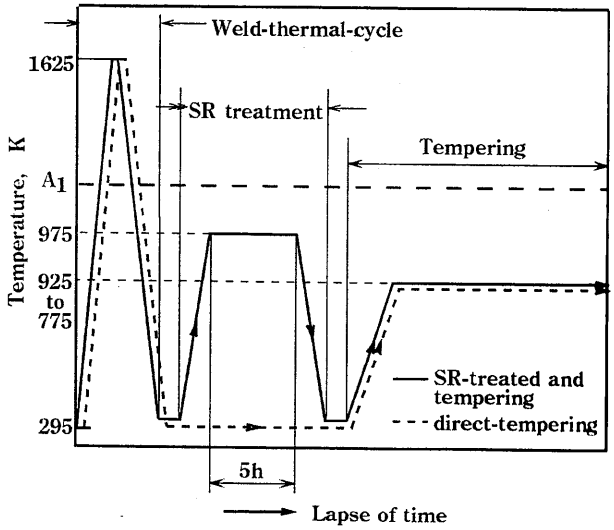


**Fig.1 Thermal histories given to the SR-treated specimen (solid line) and those to the original HAZ specimen (dotted line).**

The temperature of the SR treatment was 975K[2]. The time of 5h was selected as follows (Fig.2). The second type of embrittlement occurred at first in the short time range. The

transition temperature $vTr_{30}$ decreased with an increment of SR time. The specimen became the de-embrittled state after the second type of embrittlement disappeared around 5h. The $vTr_{30}$ as low as 113K was attained at time of 5h. However, the fifth type of embrittlement (SR embrittlement) appeared in the long time range[3].

After SR treatment, the specimen was tempered for 1h to 10000h at 775K to 925K.

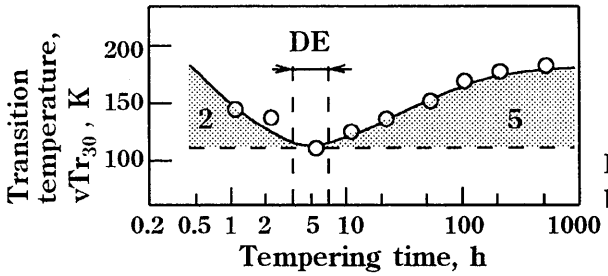


**Fig.2 De-embrittled state, DE, obtained by SR treatment for 5h at 975K.**

2.3 Detection of temper embrittlement

The half-sized Charpy impact test specimen was made from the tempered specimen. The impact test was carried out on each tempering condition by changing the testing temperature from 100K to 300K, and the transition curve was drawn. The temperature at which the specimen was fractured absorbing 30ft-lb (40.6J) of energy was adopted as the transition temperature, $vTr_{30}$. The temper embrittlement was detected as the rise of $vTr_{30}$ from the de-embrittled state[4].

## 3. Classification of temper embrittlement

### 3.1 Detection by the rise of transition temperature

Fig.3(a) shows the $vTr_{30}$-tempering time curves of direct-tempered specimens. It is assumed here that the basic $vTr_{30}$ in the non-embrittled state falls with the progress of tempering as the dotted line in the figure[1]. Each rise of $vTr_{30}$ from the non-embrittled value informs that each of different type of embrittlement occurs. The first to the fourth types of embrittlement are observed at the hills labeled "1" to "4". The figures, $S_2$ to $S_4$ and $S_D$, respectively, show the time periods at which the second to the fourth types of embrittlement and the de-embrittled state begin to arise.

At 825K, the first to the fourth types appear in order with the lapse of time (Fig.3(a3)). At 875K, the second type, de-embrittled state and the fourth type appear in order (Fig.3(a2)).

Fig.3(b) shows the change of $vTr_{30}$ of the SR-treated specimens. The dotted line in this figure shows the $vTr_{30}$ of de-embrittled state (113K) obtained by the SR treatment for 5h at 975K.

The de-embrittled state was kept in short time range. The first type of embrittlement, which occurs when martensite in the original HAZ specimen was decomposed[5,6] does not arise in the SR-treated specimens. But some hills of $vTr_{30}$ observed in the long time range informs that certain types of embrittlement is to arise there (Fig.3(b1) to (b4). The type of embrittlement was identified by the referring the results in the previous study as explained in the following sections[1].

At 775K and 825K, except for the first type, the same types of embrittlement as that in the original HAZ specimens appear. At 875K, the fourth type of embrittlement appears from $S_4$. At 875K and 925K, the second type does not appear any longer.

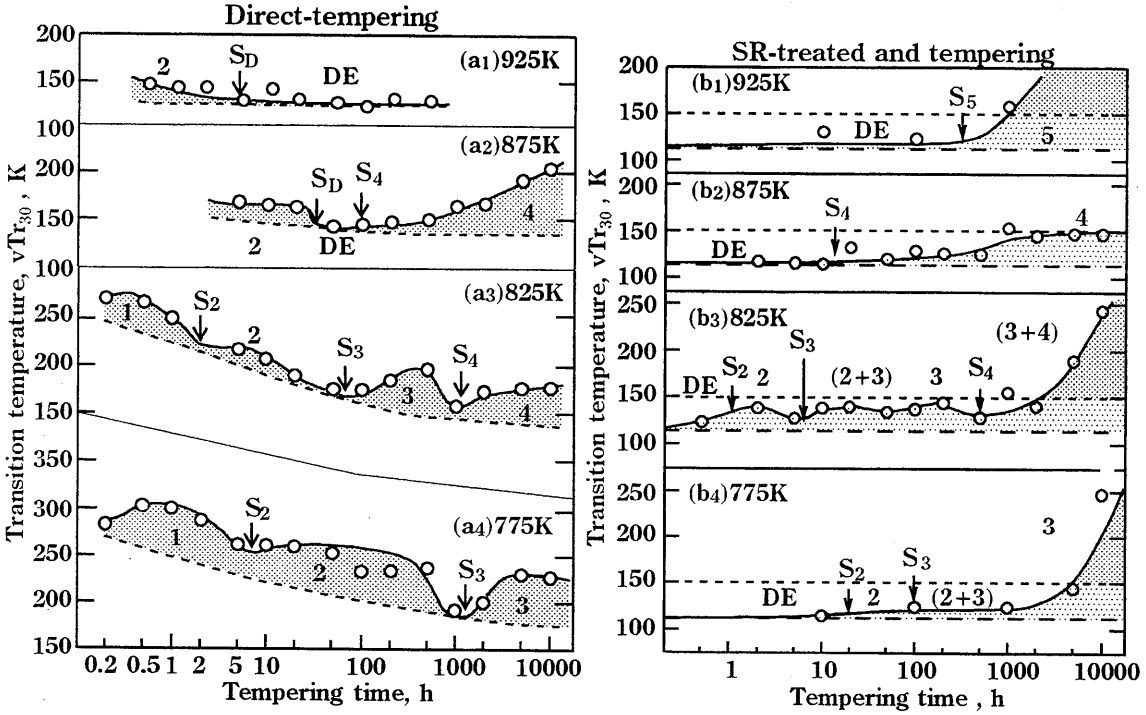


**Fig.3 Temper embrittlement observed as the rise of vTr30 in the direct-tempered(a) and the SR-treated spesimens(b).**

The high temperature type of embrittlement, the fifth type[1], is observed at 975K in the original HAZ specimen. This type appears from $S_5$.

The temper embrittlement except for the first type of embrittlement arises by SR-tempering, but the transition temperature $vTr_{30}$ in short time range is decreased significantly by SR treatment. SR treatment suppresses effectively temper embrittlement which occurs in short time range.

3.2 Shape of transition curve

The shape of transition curve of the SR-treated specimen (SRT) was compared with that of direct-tempering as shown in Fig.4.

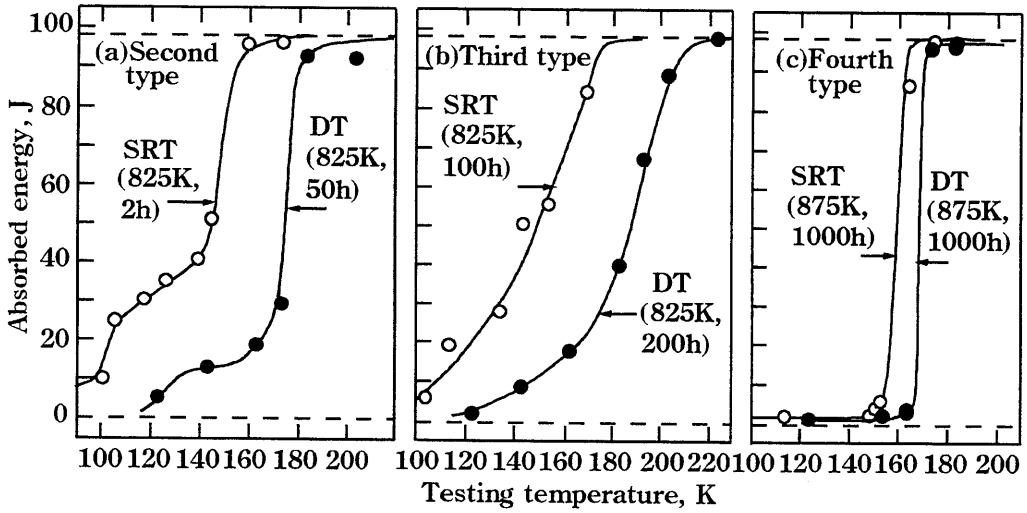


**Fig.4 Typical shapes of transition curves of the second, the third and the fourth types of embrittlement in the direct-tempered (DT) and the SR-treated specimens (SRT).**

In the second type, a stepwise transition is observed (Fig.4(a)). A slant transition occurs in the third type (Fig.4(b)). A unique vertical transition is observed in the fourth type (Fig.4(c)). These results inform that each types of embrittlement which was labeled tentatively in Fig.3(b), is identical to those in the direct-tempered one.

3.3 Fracture mode

In case of the direct-tempering, the second and the fourth types of embrittlement produced the cleavage fracture and the third type did the intergranular fracture[1].

The fracture surfaces of the impact-tested specimens which were broken below the transition temperature were observed by a SEM. Fig.5 shows the brittle fracture mode of each type of embrittlement. The cleavage fracture was observed in the time range where the second, the fourth and the fifth types arose. The intergranular fracture was observed in the time range where the third type arose. Those fracture modes meet well those observed in the direct-tempered specimens.

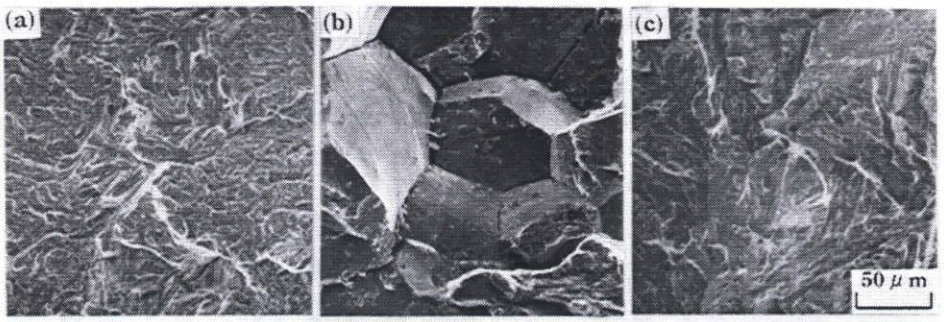


**Fig.5 Fracture surfaces of specimens in the embrittled states of (a) the second, (b)the third and (c)the fourth types.**

3.4 Time-temperature-embrittlement diagram

The time (t)-temperature (T) fields in which four types of embrittlement arise are shown in Fig.6(a). 1/T and log t are taken in the main vertical and horizontal axes of normal spacing: T(K) and t(h) are also shown in the corresponding positions. The boundary lines in this figure are drawn by using the tempering parameter, P[7].

$P=T(\log t+18)$

The fields of those types in the direct-tempered specimens are referred in Fig.6(b)[1].

The second type of embrittlement appears after SR treatment only slightly in the limited temperature range below 860K. Third type arises as well after SR treatment in the temperature range around 825K. It has been reported that the third type arises in the tempering of de-embrittled specimen as well as in the direct tempering of quenched one[8]. The field of an intensive embrittlement of this type, which exhibits the $vTr_{30}$ more than 150K (Fig.2(b3) and (b4)), is observed only in the limited time range longer than 1000h at 825K which is shown shaded area marked by "Em" in Fig.6(a).

The fourth type still arises in the same time-temperature range as that in direct-tempered specimens, however, the SR treatment reduces its intensity ($vTr_{30}$ lower than 150K: Fig.3(b2)). The fifth type which is known as SR embrittlement[9] arises when the tempering temperature is as high as 925K (Fig.6(a) and (b)).

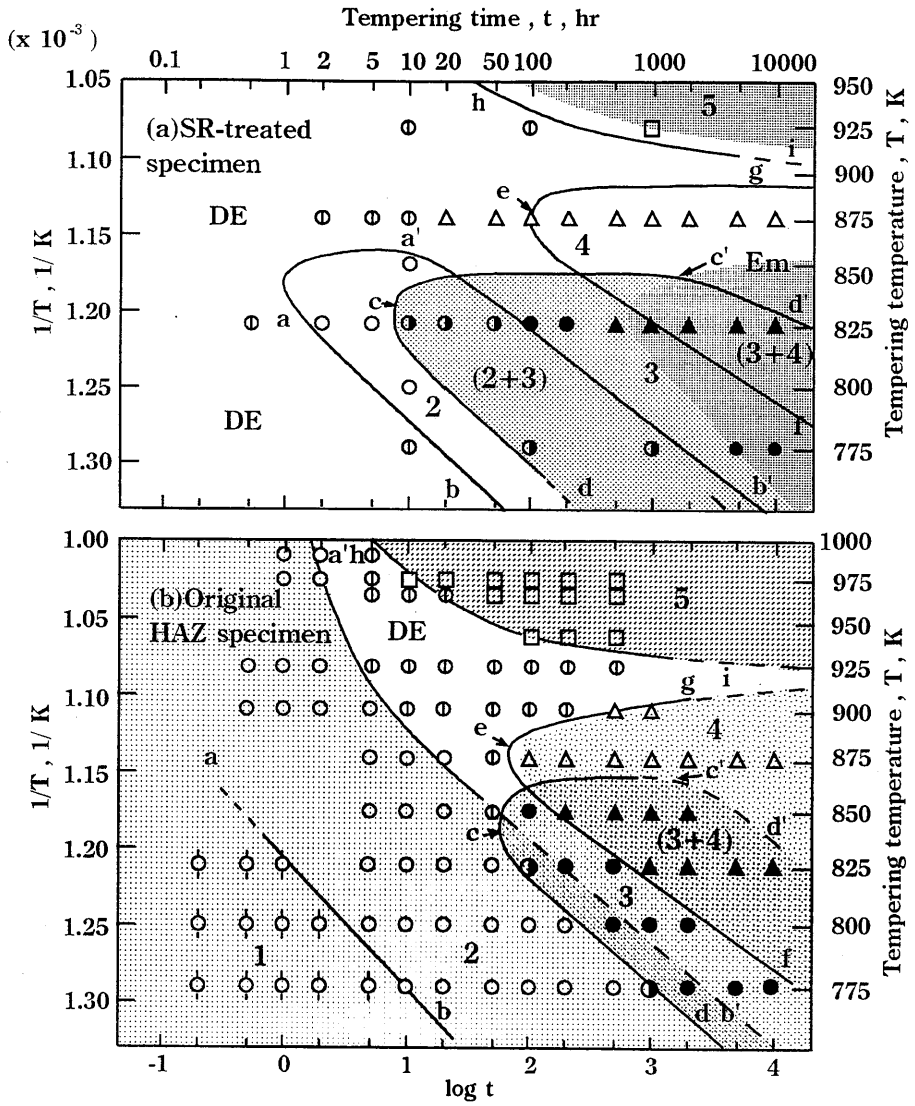


**Fig.6 Time-temperature fields in which the first to the fifth types of temper embrittlement arise; ⊖ first type, ○ second type, ◑ second and third type, ● third type, △ fourth type, ▲ third and fourth type, □ fifth type, ⊕ de-embrittled state, Em: embrittled intensively.**

4. Effect of SR treatment on the intensity of embrittlement

4.1 Third type of embrittlement

SR treatment reduces the transition temperature $vTr_{30}$ of the HAZ as explained qualitatively in the preceding chapter. Fig.7(a) shows qualitatively the effect of SR treatment on the $vTr_{30}$ in the time ranges of the second and third types of embrittlement. The $\Delta vTr_{30}$ is the difference between the $vTr_{30}$ of the direct-tempered specimens and that of the SR-tempered specimens. Fig.7(b) shows the fraction of area of intergranular fracture which accompanies to the third type by referring to that of the direct-tempered specimens (Fig.7(c)).

The SR treatment reduces the $vTr_{30}$ as much as 150K by removing the first type and partially the second type. However, in the time range in which the third type arises, the $\Delta vTr_{30}$ is reduced with the lapse of time, and at 1000h, the $vTr_{30}$ of the SR-treated specimen exceeds that of the direct-tempered one. This tendency is illustrated well by the change in the fraction of area of the intergranular fracture (Fig.7(b) and (c)).

The $vTr_{30}$ values in the time-temperature range where the third type arises are shown schematically in Fig.8 referring to those of the direct-tempered specimens (dotted line).

Although, the third type begins to arise in the earlier time range, it becomes very intensive (the $vTr_{30}$ higher than 200K) in the long time range as long as 1000h.

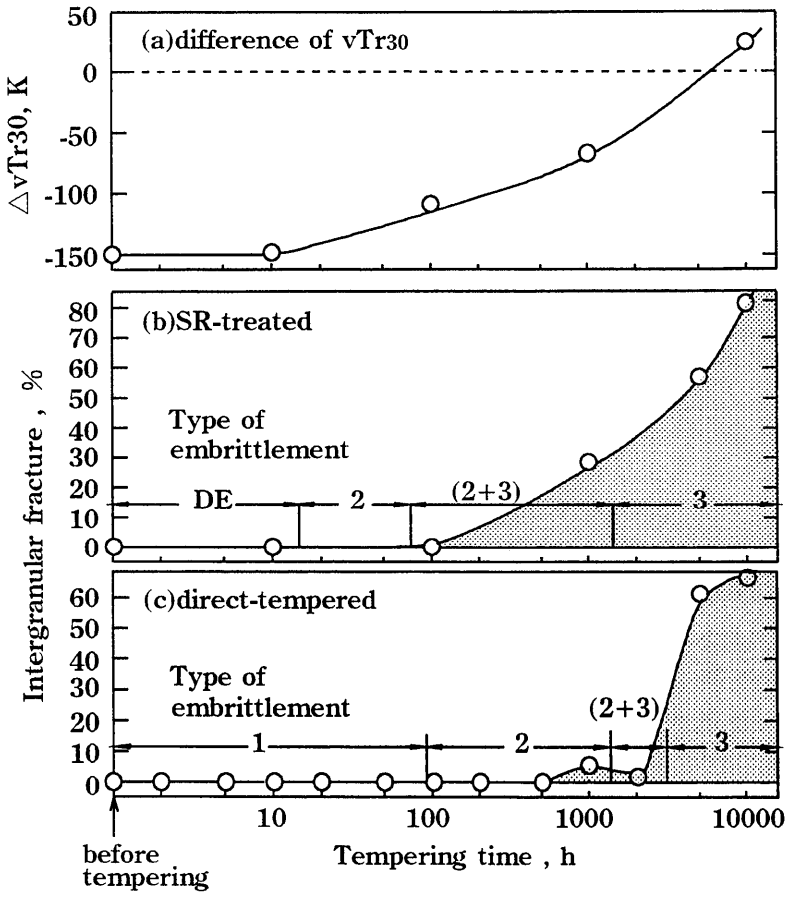


Fig.7 Difference of transition temperature, △vTr30 and the area of intergranular fracture between SR-treated and direct-tempered specimens in the time range where the third type arises; tempered at 775K.

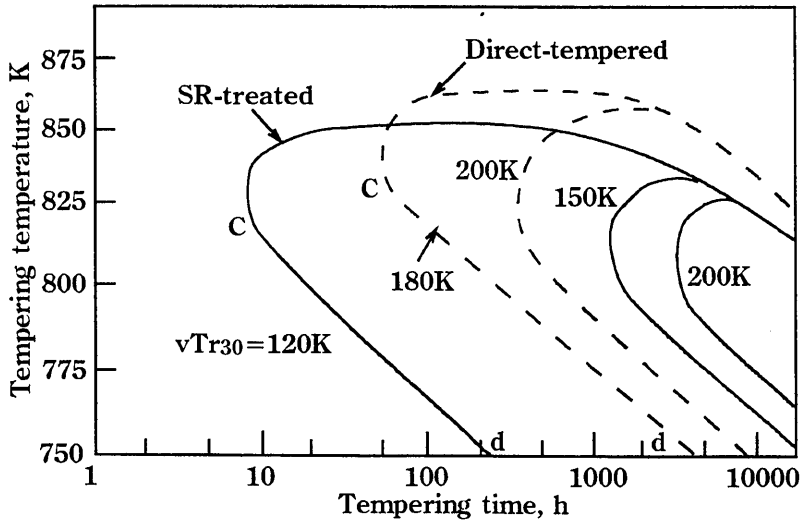


Fig.8 Time-temperature fields of the third type of embrittlement in which the $vTr_{30}$ is indicated; cd: the begining time period of the third type.

4.2 Fourth type of embrittlement

Fig.9 shows the effect of SR treatment on the $vTr_{30}$ in the time range of the fourth type of embrittlement. The rise of $vTr_{30}$ is suppressed effectively by SR treatment.

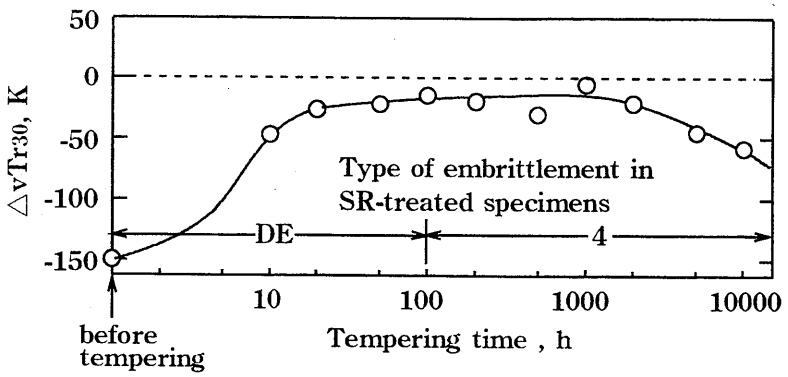


**Fig.9 Differences of transition temperature, $\Delta vTr_{30}$ between SR-treated and direct-tempered specimens in the time range where the fourth type arises; tempered at 875K.**

5. Metallurgical factors affecting the embrittlement

5.1 Effect of phosphorus concentration in grain boundary on third type

5.1.1 EDX micro-analysis on grain boundary

The phosphorus concentration in the prior-austenite grain boundary was measured on the SR-treated specimens by the EDX micro-analysis. The procedure of micro-analysis is as follows.

The prior-austenite grain boundary was revealed by etching with the saturated aqueous solution of picric added by a wetting regent[10]. A pair of indentations were made across one grain boundary as shown in Fig.10(a). The specimen was polished again to erase the groove of the grain boundary was erased as shown in Fig.10(b). The point analysis was made on 15 spots at each intervals of 70nm crossing one grain boundary. The conditions of EDX micro-analysis are as follows. Accelerate voltage; 15kV, magnification of SEM; 30000, measurement time; 50s.

The X-ray spectrum of for an element is shown in Fig.11. The intensity of an element Ie was measured as $I_{mes} - I_{bg}$. The energy ranges for measure ($E_l$ to $E_u$) are defined for P and Fe as 1.09-2.18keV and 6.18-6.64keV, respectively. The X-ray intensities in the energy range were integrated to obtain the $I_P$ and $I_{Fe}$. The phosphorus concentration in grain boundary $[P]_{mes}$ was obtained by $I_P/(I_P + I_{Fe})$.

5.1.2 Change in $[P]_{gb}$ by tempering

The $[P]_{mes}$ of as-welded HAZ, SR-treated and tempered specimens are shown in order in Fig.12(a). The phosphorus concentration in grain boundary, $[P]_{gb}$ can be expressed by the curved line with the assumption that the maximum value among each set of $[P]_{mes}$ exhibits the $[P]_{gb}$.

The $[P]_{gb}$ is already as large as 0.6mass% in the as-welded state due to the welding-induced segregation by $\alpha/\gamma$ transformation during the heating process of welding. This phenomenon has been introduced in detail in the paper of the authors[11]. SR treatment reduces the $[P]_{gb}$ to 0.2 mass%. This $[P]_{gb}$ value is kept for 100h, after that it increases reaching

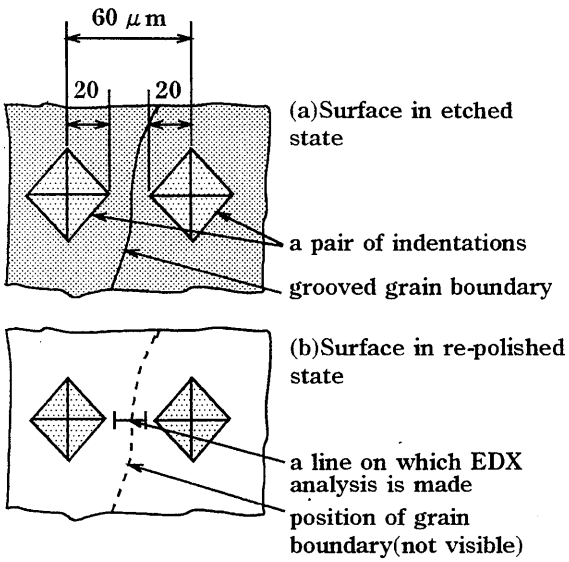


Fig.10 The grain boundary for X-ray point analysis marked by a pair of incidentes.

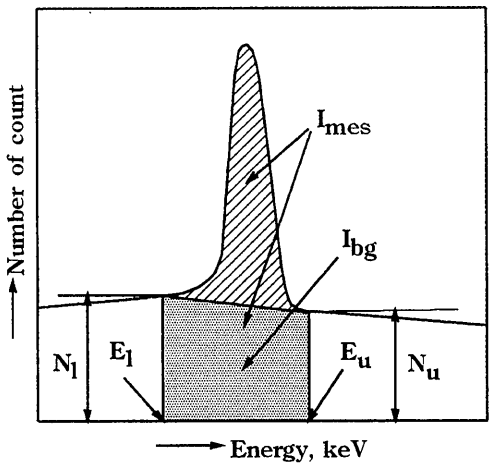


Fig.11 Determination of X-ray intensity of an element, $I_e(=I_{mes}-I_{bg})$.

the maximum value of 0.6 mass% at 1000h, and then decreases.

The change of the $[P]_{gb}$ in Fig.12(a) meets well that of the fraction of intergranular fracture of the specimens as shown in Fig.12(b). Those results inform that the third type of embrittlement is caused by the segregation of phosphorus during tempering for as long as 1000h.

The increasing process of $[P]_{gb}$ will be explained as the process of equilibrium segregation proposed by McLean[12]. However, the mechanism of the decreasing process of $[P]_{gb}$ is not yet clear at present.

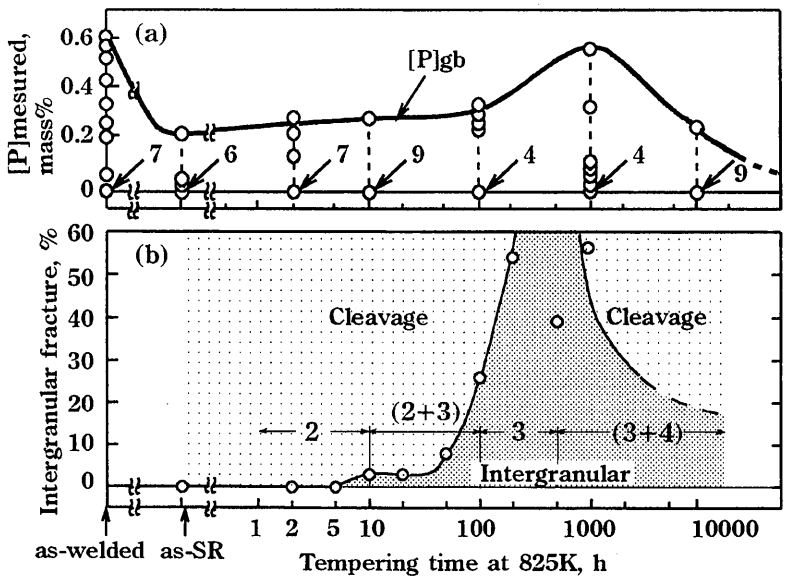


Fig.12 Changes in the phosphorus concentration in grain boundary, [P]gb (a) and the fraction of intergranular fracture (b) with the lapse of time at 825K; Figures 4 to 9 show that 4 to 9 plots are piled up on the same position.

5.2 Effect of carbide particles on the fourth type

The change in the average size of a carbide particle is shown for the time range where the fourth type arises as in Fig.5(a). The growth of carbide particles is observed in the time range as long as 1000 to 10000h in which the fourth type appears (Fig.5(b)). This result informs

that the fourth type will depends on the growing process of carbide particles[3,5]. However, the growth rate of carbide particles and hence, the rise of $vTr_{30}$ is smaller than those of the direct-tempered specimen. This result will depend on the fact that carbide particles have already grown in some extent by the SR treatment at 975K, and growth rate at the tempering temperature of 875K remains in a limited range.

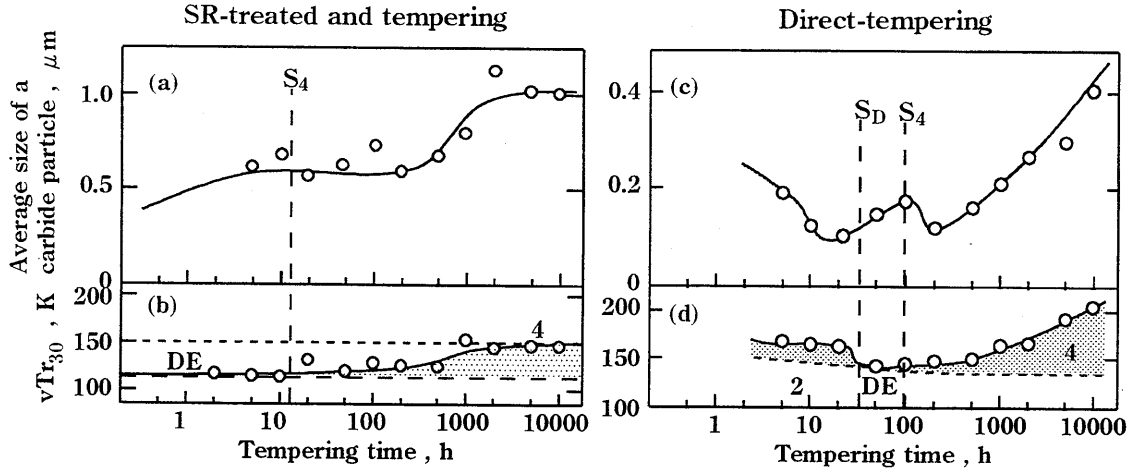


**Fig.13 Growth of carbide particles when the fourth type arises; 875K**

6. Conclusions

(1) The SR treatment at 975K for 5h makes the as-welded HAZ specimen the de-embrittled state. Some types of embrittlement are revived by tempering.
(2) In SR-treated specimens, the first type does not appear. The second and the fourth types appears a little.
(3) The third type appears slightly and significantly in the long time range.
(4) The third type, which produces the intergranular fracture, is induced by the segregation of phosphorus in the grain boundary of prior-austenite.
(5) The fourth type, which produces the cleavage fracture, will be induced by the growth of carbide particles.

References

[1]K. Tamaki, J. Suzuki, H. Kawakami et. al., *SR Embrittlement and Temper Embrittlement Observed in HAZ of 2 1/4Cr-1Mo Steel*, Res. Rep. of the Fac. of Eng. Mie. Univ., Vol.20, pp.25-40, Dec., 1995.

[2]Japan Welding Soc., *Yosetsu-setsugo Binran (Welding Handbook)*, Maruzen, pp.917-920, 1990, (Japanese).

[3]H. Kawakami, K.Tamaki et. al., *Quantifying Carbide Particles in Steel by Image Processing Method*, Res. Rep. of the Fac. of Eng. Mie. Univ., Vol.25, pp.1-15, Dec., 2000.

[4]S. Sawada and T. Ohhashi, Tetsu to Hagane, *The De-embrittlement Behavior of a Temper-embrittled Low Alloy Steel*, Vol.62, No.6, pp.644-651. June, 1976, (Japanese)

[5] H. Kawakami, K. Tamaki, J. Suzuki et. al., *Causes of Temper Embrittlement in HAZ arising in the Temperature Range below 900K*, Quarterly J. Japan Welding Soc. Vol.19, No.2, p.326-335, May, 2001, (Japanese).

[6]K. Tamaki, H. Kawakami et. al., *Influence of Metallurgical Factors on Temper Embrittlement in HAZ of Cr-Mo Steel*, Res. Rep. of the Fac. of Eng. Mie. Univ., Vol.22, pp.11-23, Dec., 1997.

[7]J.H. Hollomon and L.D. Jaffe, *Time-temperature Relation in Tempering Steel*, Trans AIME, Iron and Steel Division, Vol.162, p.223-249, 1945.
[8]H. Kawakami, K. Tamaki, J. Suzuki et. al., *Temper embrittlement in the HAZ of 2 1/4Cr-1Mo steel induced by reheating after SR treatment*, Welding International, Vol.13, No.2, pp.19-27, Feb., 1999.
[9]M. Katsumata, K. Koide, H. Kaji, *Change in Mechanical Properties with Stress Relief Annealing in Pressure Vessel Steels*, Tetsu to Hagane, Vol.75, No.2, pp.353-360, Feb., 1989, (Japanese).
[10]T. Ogura, A. Makino, T. Masumoto, *Study on the Grain Boundary Etching Method (GEM) as a Technique Analyzing the Amount of P Segregation at Grain Boundaries*, J. Japan Inst. Metals, Vol.45, No.10, pp.1093-1101, Oct., 1981,(Japanese).
[11]K. Tamaki, J. Suzuki, H. Kawakami et. al., *Phosphorus Segregation in Grain Boundary Induced by α/γ Transformation during Welding*, Quarterly J. Japan Welding Soc. Vol.19, No.1, p.60-69, Feb., 2001, (Japanese).
[12]D. McLean: *Grain Boundary in Metals*, Oxford Univ. Press (1957), p.117.